Piekarek, M., Bonneau, D., Miki, S., Yamashita, T., Fujiwara, M., Sasaki, M., ... Thompson, M. G. (2017). High-extinction ratio integrated photonic filters for silicon quantum photonics. Optics Letters, 42(4), 815-818. DOI: 10.1364/OL.42.000815

Optics Letters

High-extinction ratio integrated photonic filters for silicon quantum photonics

Mateusz Piekarek,[1,*] Damien Bonneau,[1] Shigehito Miki,[2] Taro Yamashita,[2] Mikio Fujiwara,[3] Masahide Sasaki,[3] Hirotaka Terai,[2] Michael G. Tanner,[4] Chandra M. Natarajan,[5] Robert H. Hadfield,[5] Jeremy L. O'Brien,[1] and Mark G. Thompson[1]

[1]Quantum Engineering Technology Labs, H. H. Wills Physics Laboratory and Department of Electrical & Electronic Engineering, University of Bristol BS8 1FD, UK
[2]National Institute of Information and Communications Technology (NICT), 588-2 Iwaoka, Kobe 651-2492, Japan
[3]National Institute of Information and Communications Technology (NICT), 4-2-1 Nukui-Kitamachi, Koganei, Tokyo 184-8795, Japan
[4]School of Engineering & Physical Sciences, Heriot-Watt University, EH14 4AS, UK
[5]School of Engineering, University of Glasgow, G12 8QQ, UK
*Corresponding author: mateusz.piekarek@bristol.ac.uk

Received 6 October 2016; revised 25 November 2016; accepted 29 November 2016; posted 1 December 2016 (Doc. ID 269910); published 13 February 2017

We present the generation of quantum-correlated photon pairs and subsequent pump rejection across two silicon-on-insulator photonic integrated circuits. Incoherently cascaded lattice filters are used to provide over 100 dB pass-band to stop-band contrast with no additional external filtering. Photon pairs generated in a microring resonator are successfully separated from the input pump, confirmed by temporal correlations measurements.

OCIS codes: (270.5585) Quantum information and processing; (130.7408) Wavelength filtering devices.

https://doi.org/10.1364/OL.42.000815

Linear optical quantum computing is a promising approach to quantum information processing. However, a practical system requires a large amount of resources [1–3]. Integrated platforms provide a solution to tackle this problem through high component density. Silicon photonics has grown rapidly in recent years to become a promising platform due to unparalleled scalability, CMOS-compatibility, and access to affordable, mature fabrication techniques. While single-photon sources based on spontaneous four-wave mixing (SFWM) have already been demonstrated [4–8], the problem of the co-propagating input pump has received very little attention. A solution is to use high-extinction ratio, low-loss, on-chip filters. Thus far, quantum photonic experiments have been performed using bulky external optical filters [9–13], which typically exhibit high transmission losses. Integration of photon sources and filters on a single chip is a key step in realizing full-scale quantum photonic circuits. Filters based on coupled resonator optical waveguides (CROW) with extinction ratios in excess of 50 dB have been demonstrated in SiN [14] and silicon-on-insulator [15,16]. The first result showing the extinction ratio of 100 dB with a total loss through the filter of 3 dB was demonstrated by [17]. However, only recently have photons been successfully generated and demultiplexed using an integrated circuit without external filtering, as shown in [18], using distributed Bragg reflectors. Here we report an alternative filter structure for high-extinction filtering. The feasibility is verified through the on-chip generation and rejection of the pump using two photonic integrated circuits. The two chips were necessary, as in the previous experiments, to suppress the background scattering.

As mentioned in the previous paragraph, silicon single-photon sources are based on SFWM. By exploiting the $\chi^{(3)}$ nonlinearity of the material, with a certain probability, two pump photons are absorbed and a non-degenerate signal-idler pair is generated. In this experiment, a microring resonator was used to generate single photons. By pumping one of the resonances with a bright light, a signal-idler pair is generated spectrally on either side of the pumped resonance. This process leads to three spectrally separated signals co-propagating at the output. Therefore, the bright pump has to be filtered out while preserving the single-photon pair.

An energy of a single photon at the telecommunication C-band wavelength is of the order of 10^{-16} mJ. Any background noise above that level degrades the signal-to-noise ratio (SNR) of the single-photon source. In a practical system, parameters such as insertion loss, source brightness, detector efficiency, and dark count levels affect the performance. For an input power of 1 mW and a dark count rate of 1 kHz (10^{-13} mW), 130 dB of pass-band to stop-band contrast is required to attenuate the pump to the detector noise level.

Lattice filters are coherently cascaded unbalanced Mach–Zehnder interferometers. The advantage over an unbalanced Mach–Zehnder interferometer (UMZI) is the high degree of control over the spectral shape of the filter [19,20]. In [21], lattice filters were cascaded to create a passive, low-loss demultiplexer. Both of these characteristics are vital for the large-scale integration of quantum photonic devices. Alternative approaches such as cavity-based filters require tuning and are sensitive to fabrication tolerances. In addition, interferometric filters rely on standard components such as directional couplers and waveguides. This greatly relaxes the requirements for fabrication, which in turn lowers the cost and improves reproducibility. Lattice filters exhibit low pass and stop-band ripples and a low insertion loss dependent only on the waveguide scattering and footprint.

Here, our on-chip filters were based on a 3rd order lattice filter presented in [21], as shown in Fig. 1. The order is defined by the maximum number of elementary delays ΔL between the two outputs. The stop-band bandwidth, which depends on the directional coupler reflectivities and the filter free spectral range, was designed to be at least 1 nm at −20 dB suppression level. Wide pass and stop-bands significantly reduce the tuning requirements for the microring source. Combined with a flat transmission, it also reduces the effect of the filter response on the spectral shape of the generated photon. A single filter stage was expected to provide up to 20 dB pass-band to stop-band contrast. Therefore, the lattice filter was incoherently cascaded to generate higher stage filters. The unwanted output of each stage was tapered out into the cladding away from the grating couplers.

The photonic integrated circuits (PICs) were fabricated by CEA-LETI in 193 nm lithography, which has been shown to produce high device uniformity [22]. Therefore, a good spectral overlap was expected between the closely placed components. However, the overlap between separate dies was not guaranteed. The layout contained separate 2-, 4-, 6-, and 8-stage cascaded 3rd order lattice filters. Four of the structures were combined with microring resonator single-photon sources with a free spectral range (FSR) of 400 GHz (corresponding to a cavity length of ≈180 μm). The FSR was designed to be 800 GHz, double that of the source. While the on-chip filters were fully passive, the microring resonator sources were thermally tunable via the on-chip heaters.

In this experiment, two silicon-on-insulator (SOI) PICs were interconnected as shown in Fig. 1. A CW beam was injected in the first chip, pumping a microring source generating correlated photon pairs, then going through a 6-stage filter attenuating the pump while letting the photon pair through. A 4-stage filter was used on the second chip to sufficiently suppress the co-propagating laser beam. To spectrally overlap the filters across the two dies, chips A and B were thermally tuned using standard peltier modules to 29.5°C and 30.6°C, respectively. The external arrayed waveguide grating (AWG) filter was used to increase the SNR of the input pump. Two polarization controllers, one before each chip, provided the required adjustment necessary to optimise the coupling. An external 50/50 fiber beamsplitter was used in order to non-deterministically split the two photons into separate arms. Superconducting nanowire single-photon detectors were used with one of the arms having an additional fiber path delay of 20 m. Optical input and output was achieved through grating couplers designed to match the 127 μm spacing of an external V-groove fiber array (VGA). Each coupler exhibited approximately 5 dB coupling loss.

Filters on the same device with 2, 4, 6, and 8 cascaded stages were characterized and compared as shown in Fig. 2. As shown in the plot, the spectral overlap and shape remained consistent with increasing order. Due to the large variation with wavelength, the signal channel exhibited between 0.5 to 1.5 dB, depending on the number of cascaded stages, more loss than the idler channel. We estimate the average loss per filter stage—calculated by subtracting the grating coupler loss from the peak transmission through the filter and dividing it by the number of stages—to be ≈0.25 dB. The noticeable increase in the transmission loss between the 4- and 6-stage filter is attributed to an imperfect spectral overlap. The single photons generated from the resonator have a longer coherence time than the cavity lifetime [23]. Estimating the Q-factor of the source to be around 90000, this translates to a coherence length in silicon of 5 mm, which is much longer than the path length difference in a single stage of the lattice filter, ensuring its proper operation.

As can be seen in the plot, the 4-stage filter provided approximately 56 dB extinction between 1550 and 1558 nm. We estimate that the 8-stage cascaded lattice filter provided at least 100 dB pass-band to stop-band contrast. However,

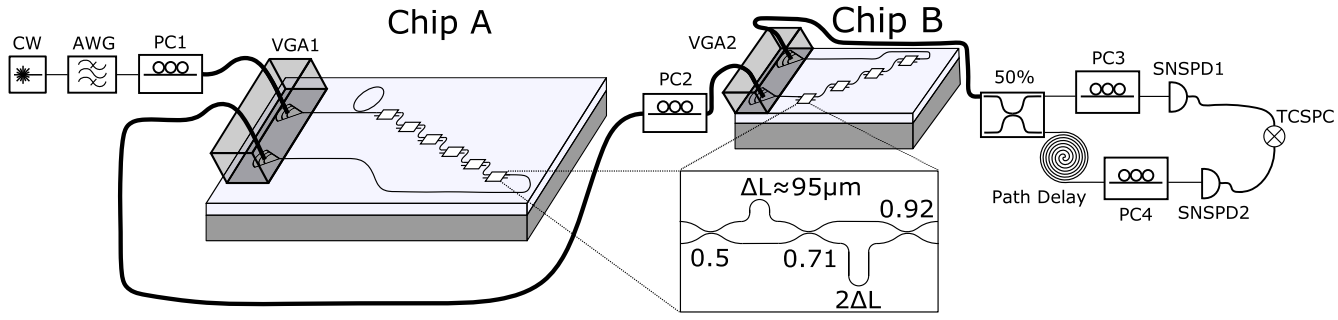

Fig. 1. Full experiment schematic showing two interconnected chips. Chip A contains a ring resonator photon pair source followed by a 6-stage pump-rejection filter. Chip B contains a 4-stage pump-rejection filter. Each stage is composed of a 3rd order lattice filter. Two types of measurements are performed. When measuring photon pairs, a CW laser is externally pre-filtered (to suppress the noise in the photon pair bandwidth) and injected in chip A. Single-photon measurements are performed after chip B using a fiber splitter to non-deterministically separate the single photons that are then routed to the single photon detectors. When looking at the spectral response of the filters, the CW laser is directly connected to the input of chip A. The output is monitored with a power-meter.

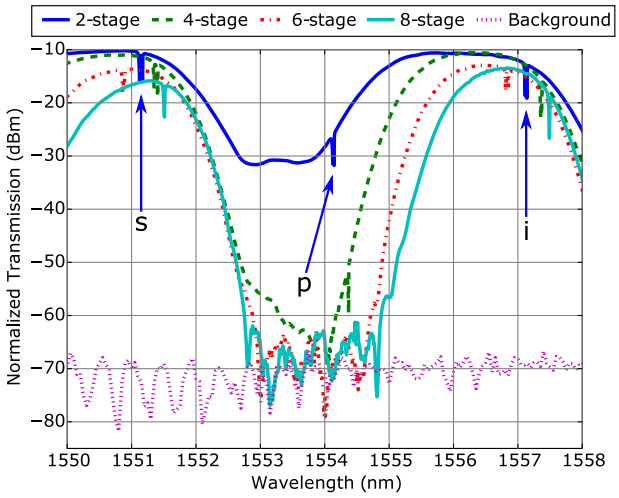

Fig. 2. Spectral response of varying stage filters on chip A. From lower to higher pass-band loss: 2-, 4-, 6-, and 8-stage filters. The bottom line represents the background light due to scattering. The annotations *s*, *i*, and *p* refer to signal and idler photons and input pump resonances, respectively. On the 6-stage filter, the pump resonance was thermally tuned to be in the stop-band—with the signal and idler being in the pass-band. None of the devices have been thermally tuned on the 2-, 4-, and 8-stage filters.

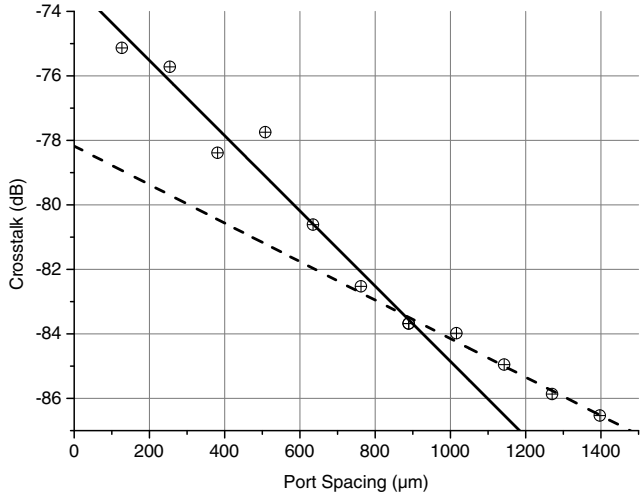

Fig. 3. Measured crosstalk level with an increasing input and output port separation. Each data point represents the average optical power of the wavelength response measured between 1540 to 1560 nm. The data is fit with two linear trends represented by the solid and dashed lines.

the measurement was limited to around −65 dB by the background noise identified as the on-chip scattering from the pump, as shown in Fig. 2—this data was taken by moving the VGA away from the grating couplers while keeping the vertical distance unchanged. To get beyond this limit and measure correlated photon pairs, two chips had to be interconnected, with each one providing approximately 65 dB of suppression of the unguided light.

The optical crosstalk was further investigated by performing a wavelength scan between 1540 and 1560 nm at different input to output port separations. A 16-port polarization maintaining VGA and a high-sensitivity photodetector were used during the measurement. The fiber array was aligned with one of the filter circuits and the output at each dark port was measured, while the light was sent through the on-chip structure. Due to the size of the chip, 11 ports were investigated. The result of the experiment is shown in Fig. 3. Two linear fits can be seen, represented by the solid and dashed lines, for closer and farther port spacings. The light scattered inside the chip should exhibit an exponential decay (linear in dB scale) with distance (solid line) due to the multiple transmissions and reflections at various interfaces. We attribute the second trend (dashed line) to the light reflected back to the fiber array directly from the chip input. This latter effect becomes dominant at larger port spacings, resulting in a reduction in crosstalk of less than 0.6 dB per 100 μm. Therefore, while increasing the distance between the input and output ports may lead to some improvement, it is not a practical solution for fully suppressing the crosstalk to the necessary levels.

By combining the 6-stage filter with a microring resonator source on chip A with the 4-stage filter on chip B, the background noise was suppressed below the detection level of the photodiode, as shown in Fig. 4. The obvious disadvantage was a significant increase in the total transmission loss through the system.

The performance of our devices was further investigated using superconducting nanowire single-photon detectors (SNSPDs). A temporal correlation measurement was performed to verify the signal and idler pair generation and the on-chip filtering. The pump source used in the experiment exhibited −100 dBm noise level. For the measurement shown in Fig. 5 the pump was pre-filtered using an external AWG filter to further increase the SNR of the input beam. The pump wavelength was 1553.84 nm, and the power injected into Chip A was 7 dBm. A coincidence peak confirms the

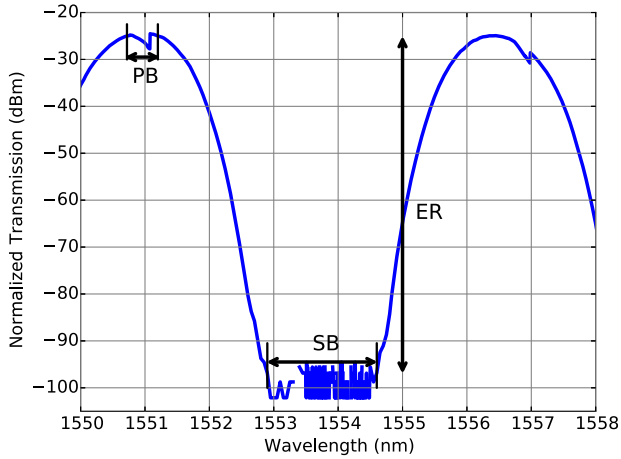

Fig. 4. Two interconnected and spectrally aligned PICs. The 6-stage cascaded lattice filter on one chip is combined with the 4-stage filter on the second chip. Microring resonator resonances are broadened due to the relatively high input power of 12 dBm. PB, SB, and ER are the pass and stop-band bandwidths and the extinction ratio, respectively. We note that the full ER could not be measured due to reaching the noise floor of the measurement apparatus.

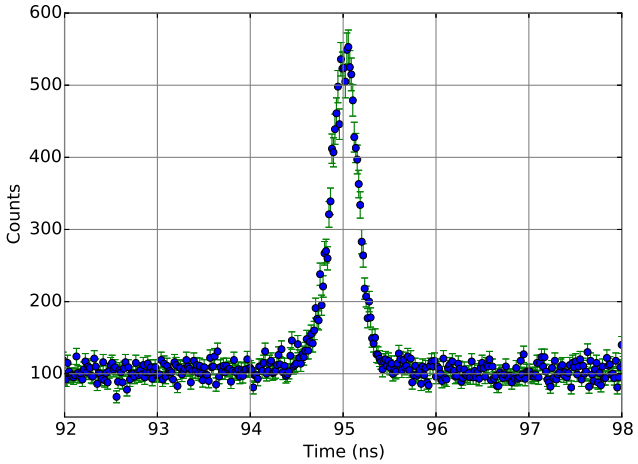

Fig. 5. Temporal correlations coincidence peak integrated over 4 h. The pump was pre-filtered using an external AWG filter. The input power to the chip was 7 dBm.

performance of both the single-photon source and the on-chip filters. In this experiment, the correlated photon pairs from across all ring resonances satisfying energy conservation, phase matching, and in the pass-band of the lattice filter were detected. However, that can be mitigated in the future chip design by adding an on-chip wavelength division multiplexer. We recorded 1.16 coincidental events per second and had an accidental background of ACC = 0.007 accidental events per second per time-bin $\tau = 16$ ps. The averaged singles per channel through the full duration of the measurement (14400 s) were $C_1 = 1.7 \times 10^4$ s^{-1} and $C_2 = 2.5 \times 10^4$ s^{-1}. We estimated them from the final readout on the time correlator single photon counter (TCSPC) and the accidentals ACC $= C_1 C_2 \tau$. We fit the coincidence histogram with a Gaussian distribution and extracted a coincidence-to-accidental ratio (CAR) of 2.5. Such a low value was caused by a combination of high transmission losses (≈25 dB), leakage of the pump photons, and the combined electronic jitter of the detectors and the counting electronics.

One other aspect which can impact the pump rejection is the polarization. Our lattice filter was designed to work only on the TE mode. In our experiment, the pump exhibited a TE to TM rejection ratio of 20 dB. The pump then went through four grating couplers in total (two per chip), each suppressing the TM mode by 20–25 dB, giving approximately 100 to 120 dB TE to TM rejection ratio comparable with the pump filter rejection of our filter.

We have demonstrated photon pair generation in a micro-ring resonator and the subsequent rejection of the co-propagating laser pump across two SOI integrated circuits fabricated with 193 nm lithography. At the pumping wavelength, Chip A and Chip B exhibited extinction ratios of around 55 dB each, as shown in Fig. 2, giving an estimate of at least 100 dB pass-band to stop-band contrast using fully passive lattice filters. Full integration of single-photon sources, filters, and detectors is limited the on-chip scattering. Future systems will have to mitigate this effect by understanding and managing the scattering in the full substrate. Our result demonstrates the resilience of the lattice filter structure to manufacturing tolerances. This approach provides an extra step toward full integration of components required to create a single-photon source, which is crucial for building a large-scale quantum computer.

Funding. Engineering and Physical Sciences Research Council (EPSRC); European Research Council (ERC) European Commission (EC) (323734).

Acknowledgment. J. L. O. acknowledges a Royal Society Wolfson Merit Award and a Royal Academy of Engineering Chair in Emerging Technologies. M. G. T. acknowledges support from an EPSRC Early Career Fellowship.

REFERENCES

1. J. L. O'Brien, A. Furusawa, and J. Vučković, Nat. Photonics **3**, 687 (2009).
2. D. Bonneau, G. J. Mendoza, J. L. O'Brien, and M. G. Thompson, New J. Phys. **17**, 043057 (2015).
3. M. Gimeno-Segovia, P. Shadbolt, D. E. Browne, and T. Rudolph, Phys. Rev. Lett. **115**, 020502 (2015).
4. J. W. Silverstone, D. Bonneau, K. Ohira, N. Suzuki, H. Yoshida, N. Iizuka, M. Ezaki, C. M. Natarajan, M. G. Tanner, R. H. Hadfield, V. Zwiller, G. D. Marshall, J. G. Rarity, J. L. O'Brien, and M. G. Thompson, Nat. Photonics **8**, 104 (2013).
5. J. E. Sharping, K. F. Lee, M. A. Foster, A. C. Turner, B. S. Schmidt, M. Lipson, A. L. Gaeta, and P. Kumar, Opt. Express **14**, 12388 (2006).
6. S. Clemmen, K. Phan Huy, W. Bogaerts, R. G. Baets, P. Emplit, and S. Massar, Opt. Express **17**, 16558 (2009).
7. C. Xiong, C. Monat, A. S. Clark, C. Grillet, G. D. Marshall, M. J. Steel, J. Li, L. O'Faolain, T. F. Krauss, J. G. Rarity, and B. J. Eggleton, Opt. Lett. **36**, 3413 (2011).
8. N. Matsuda, H. Takesue, K. Shimizu, Y. Tokura, E. Kuramochi, and M. Notomi, Opt. Express **21**, 8596 (2013).
9. A. Politi, M. J. Cryan, J. G. Rarity, and J. L. O'Brien, Science **320**, 646 (2008).
10. J. C. F. Matthews, A. Politi, A. Stefanov, and J. L. O'Brien, Nat. Photonics **3**, 346 (2009).
11. D. Bonneau, E. Engin, K. Ohira, N. Suzuki, H. Yoshida, N. Iizuka, M. Ezaki, C. M. Natarajan, M. G. Tanner, R. H. Hadfield, S. N. Dorenbos, V. Zwiller, J. L. O'Brien, and M. G. Thompson, New J. Phys. **14**, 045003 (2012).
12. N. Matsuda, P. Karkus, N. Hidetaka, T. Tsuchizawa, W. J. Munro, H. Takesue, and K. Yamada, Opt. Express **22**, 22831 (2014).
13. E. Murray, D. P. Ellis, T. Meany, F. F. Floether, J. P. Lee, J. P. Griffiths, G. A. C. Jones, I. Farrer, D. A. Ritchie, A. J. Bennet, and A. J. Shields, Appl. Phys. Lett. **107**, 171108 (2015).
14. M. A. Popović, T. Barwicz, M. R. Watts, P. T. Rakich, L. Socci, E. P. Ippen, F. X. Kärtner, and H. I. Smith, Opt. Lett. **31**, 2571 (2006).
15. P. Dong, N. N. Feng, D. Feng, W. Qian, H. Liang, D. C. Lee, B. J. Luff, T. Banwell, A. Agarwal, P. Toliver, R. Menendez, T. K. Woodward, and M. Asghari, Opt. Express **18**, 23784 (2010).
16. X. Luo, J. Song, S. Feng, A. W. Poon, T. Y. Liow, M. Yu, G. Q. Lo, and D. L. Kwong, IEEE Photon. Technol. Lett. **24**, 821 (2012).
17. J. R. Ong, R. Kumar, and S. Mookherjea, IEEE Photon. Technol. Lett. **25**, 1543 (2013).
18. N. C. Harris, D. Grassani, A. Simbula, M. Pant, M. Galli, T. Baehr-Jones, M. Hochberg, D. Englund, D. Bajoni, and C. Galland, Phys. Rev. X **4**, 041047 (2014).
19. C. K. Madsen and J. H. Zhao, *Optical Filter Design and Analysis: A Signal Processing Approach* (Wiley, 1999).
20. K. Yamada, T. Shoji, T. Tsuchizawa, T. Watanabe, J. I. Takahashi, and S. I. Itabashi, Opt. Lett. **28**, 1663 (2003).
21. F. Horst, W. M. Green, S. Assefa, S. M. Shank, Y. A. Vlasov, and B. J. Offrein, Opt. Express **21**, 11652 (2013).
22. S. K. Selvaraja, W. Bogaerts, P. Dumon, D. Van Thourhout, and R. Baets, IEEE J. Sel. Top. Quantum Electron. **16**, 316 (2010).
23. L. G. Helt, Z. Yang, M. Liscidini, and J. E. Sipe, Opt. Lett. **35**, 3006 (2010).